Expectation Maximization (EM)과 Least Mean Square (LMS) algorithm을 이용하여 초음파 비파괴검사 신호의 분류를 하기 위한 새로운 접근법

A novel approach to the classification of ultrasonic NDE signals using the Expectation Maximization (EM) and Least Mean Square (LMS) algorithms

김 대 원
Daewon Kim

요 약

초음파 검사 방법은 여러 가지 물질들의 흠집이나 틈새, 그리고 티끌 등을 감지해내는데 널리 쓰이고 있다. 그 중 초음파 신호를 분석하는 절차는 전체의 신호처리 과정에서 아주 중요한 역할을 담당하고 있다. 많은 초음파 신호처리와 신호분류의 방법들이 제기 되었는데 그 중 가장 널리 쓰이는 방법은 신호들의 특징 공간 상에서 그 특정의 성분들을 추출해내고 그 후 신경망 네트웍을 통한 분류 방법을 이용하여 초음파 신호들을 구별해 내는 방법이다. 이 논문은 기존의 신호 분류 체계와는 다른 대체 신호 분류법을 제시하고 있는데 이것은 최소 평균 제곱 (LMS) 알고리즘을 이용하여 핵 전력 발전소에서 쓰이는 증기 발생기 튜브로부터 감지되어진 초음파 비파괴 검사 신호 (ultrasonic nondestructive evaluation signal) 을 분류해내는데 쓰일 수가 있다. 이 초음파 비파괴 검사 신호는 튜브내의 흠집이나 틈새로부터 감지되어진 신호일수도 있고 또는 튜브내의 침전물에 의해서 발생된 신호일 수도 있는데 이 두가지 신호는 매우 유사하기 때문에 반드시 분류를 해내어 침전물에 의한 신호일 경우는 무방하지만 흠집이나 갈라진 틈새에서 나오는 신호일 경우는 더 이상의 오염이나 사고 등을 방지하기 위해 수리 또는 교체 등의 후속 조치로 이어져야 한다. 이러한 절차를 밟기 위하여 증기 발생기 튜브의 내부에서의 초음파 센서로부터 증기 발생기 튜브 사이의 거리를 측정하는데 모델링 기법에 기반한 deconvolution 방법이 제시되었고 여기서 나온 결과가 정리, 분석되었다. 이 방법은 space alternating generalized expectation maximization (SAGE) 알고리즘을 이차원 미분 파라미터인 Hessian의 사용으로 인하여 수렴속도가 빠른 Newton-Raphson 알고리즘과 함께 병행 사용하여 초음파 신호의 초점 도달 시간과 그 크기를 측정하여 초점 도달 거리에 따라 두종류의 신호를 분류, 차별화 하는 기법이다. 이 알고리즘을 이용한 접근법으로 얻어진 결과가 흠집이나 틈새로부터 나온 신호일 경우와 퇴적물에 의해 나온 신호일 경우로 정리, 분류되었고 적절한 분류 효과를 보인 결과가 이 논문에 제시되었다.

Abstract

Ultrasonic inspection methods are widely used for detecting flaws in materials. The signal analysis step plays a crucial part in the data interpretation process. A number of signal processing methods have been proposed to classify ultrasonic flaw signals. One of the more popular methods involves the extraction of an appropriate set of features followed by the use of a neural network for the classification of the signals in the feature space. This paper describes an alternative approach which uses the least mean square (LMS) method and expectation maximization (EM) algorithm with the model based deconvolution which is employed for classifying nondestructive evaluation (NDE) signals from steam generator tubes in a nuclear power plant. The signals due to cracks and deposits are not significantly different. These signals must be discriminated to prevent from happening a huge disaster such as contamination of water or explosion. A model based deconvolution has been described to facilitate comparison of classification results. The method uses the space alternating generalized expectation maximization

(SAGE) algorithm in conjunction with the Newton-Raphson method which uses the Hessian parameter resulting in fast convergence to estimate the time of flight and the distance between the tube wall and the ultrasonic sensor. Results using these schemes for the classification of ultrasonic signals from cracks and deposits within steam generator tubes are presented and showed a reasonable performances.

Key words : Ultrasonic signals, Classification, NDE, EM, LMS, SAGE, SAFT, Newton-Raphson method.

I. Introduction

It has long been recognized that there is a need to inspect machines and materials around people in order to prevent failures. For example, gas pipelines buried underground are needed to be inspected regularly to minimize the possibility of catastrophic failures due to the weakening effects of corrosion on the pipe. Most NDE techniques involve the application of some form of energy to the specimen. A snapshot of the interaction between the material and energy is taken and analyzed to determine the state of the specimen. Ultrasonic and electromagnetic energy are some of the typical forms of energy that are employed to interrogate the test specimen [1]. The choice of the specific NDE method depends on many factors including the size, orientation and location of the flaw, as well as the type of material, etc [2]. Ultrasonic testing is a versatile NDE method which is employed for testing a wide variety of materials. Using this method, cracks, inclusions and other kinds of anomalies can be detected even when they exist deep within the test specimen. Ultrasonic testing uses high frequency acoustic waves ranging from 1 to 10 mega Hertz (MHz) which are typically generated using piezoelectric transducers [3]. The ultrasound wave from the transducer propagates through the material. Ultrasound waves, in general, are classified on the basis of the mode of vibration of the particle of the medium with respect to the direction of propagation of the waves, namely longitudinal, transverse (or shear), and surface waves. Longitudinal waves are the most common form of sound where the oscillations occur in the longitudinal direction. In this wave, alternate compression and rare faction zones are produced by the vibration of the particles parallel to the direction of the propagation of the wave. In the case of transverse or shear waves, the direction of particle displacement is at right angles or transverse to the direction of propagation. For these kinds of waves to travel through a material, it is necessary for each particle of the material to be strongly bound to its neighbors so that it pulls its neighbor with it as it moves. Surface waves can travel only along a surface bounded on one side by strong elastic forces of the solid. These waves have a velocity of approximately 90% that of shear waves in the same material [3]. The ultrasonic testing method is capable of providing quantitative information regarding the thickness of the component, depth of an indicated discontinuity, the size of the discontinuity, etc. Many types of pulse-echo ultrasonic flaw detectors are commercially available. For a flaw detector, three essential working units are needed in addition to a power supply and a personal computer (PC) to acquire and save the ultrasonic data. Typical equipment include a pulse transmitter, receiver-amplifier and cathode-ray oscilloscope. Figure 1 shows the block diagram of a typical ultrasonic NDE system [4].

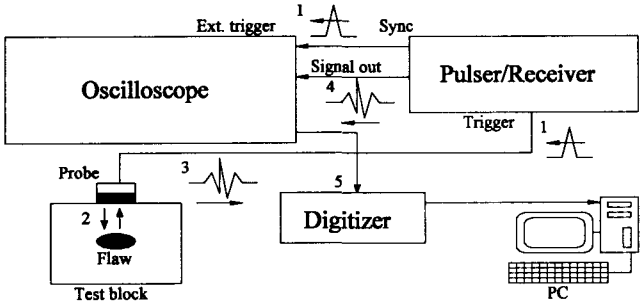

Fig. 1. Typical setup for ultrasonic NDE system

The pulse transmitter generates a high voltage spike which sets the transducer into oscillation and the trigger pulse for starting the oscilloscope display. There will be an initial pulse called *big bang* or *main bang*, which results from the high voltage spike striking the transducer. Once the spike is released, the pulse transmitter becomes an open nonconducting electrical circuit while the receiving circuit is waiting for the return signal to strike the transducer. If there are no discontinuities present, the back echo would result from the pulse traveling through the test specimen, reflecting off of the end, and returning to the

transducer. The back echo is picked up by the transducer and converted into an electrical signal whose magnitude is smaller than the transmitted pulse, so it must be amplified and filtered before it is used for any purpose. The ultrasonic data can be presented in various types. Commonly, A-Scan, B-Scan and C-Scan types are used. An A-Scan displays the echoes like an ordinary oscilloscope. In this type of display, the X-axis represents time of flight (TOF) of the pulses converted into distance traveled by the pulses while the Y-axis represents the amplitude of the echoes. The B-Scan presentation gives a cross sectional view of the part being tested and shows the length and depth of a flaw in the test material. When moving the transducer along a straight line on the surface of the test material, the displacement of the transducer can be converted into an electrical signal and this value is displayed along the X-axis and the travel of the ultrasonic pulse in the test material is represented by the time base moving the spot along the Y-axis. The C-Scan display is a plan view with horizontal and vertical positions of flaws. In other words, the discontinuity echoes are displayed as a top view of the test surface. In this display mode, X- and Y-axes are both in the plane of the surface of the test object. Other types of display modes are also used in industry such as D-, F-, and P-Scans [5]. Aamir [6] proposed a classification system that classifies the cracks from deposits formed on the steam generator tubes. Stages involved in the classification process include pre-processing of the B-Scan signals, feature extraction and selection, and classification using a neural network. The features were extracted using the discrete wavelet transform and the coefficients were applied to a multi-layer perceptron neural network that was trained using the well-known backpropagation learning algorithm. Feder [7] developed a computationally efficient algorithm for parameter estimation of superimposed signals based on the expectation maximization (EM) algorithm. The objective is to decompose the observed data into their signal components and then to estimate the parameters of each signal component separately. Fessler [8] described the space alternating generalized expectation maximization (SAGE) algorithm, which updates the parameters sequentially by alternating between several small hidden-data spaces defined by the algorithm designer. Demirli [9][10] presented a generalized parametric ultrasonic echo model, composed of a number of Gaussian echoes corrupted by noise, and algorithms for accurately estimating the parameters. The merits of the model-based estimation method in ultrasonic application has been explored. In this paper, a model based deconvolution has been described to facilitate comparison of classification results. The method uses the space alternating generalized expectation maximization (SAGE) algorithm in conjunction with the Newton-Raphson method which uses the Hessian parameter resulting in fast convergence to estimate the time of flight and the distance between the tube wall and the ultrasonic sensor. Results using these schemes for the classification of ultrasonic signals from cracks and deposits within steam generator tubes are presented and showed a reasonable performance.

II. Ultrasonic NDE of Steam Generator Tubes in a Nuclear Power Plant

Steam generators are used for converting water into steam from heat produced in the reactor core in a nuclear power plant. Figure 2 shows a typical steam generator. Each steam generator contains approximately 3,000 to 16,000 tubes through which hot radioactive water flows through. Heat is conducted through the tube wall to a mixture of water and steam outside of the tube.

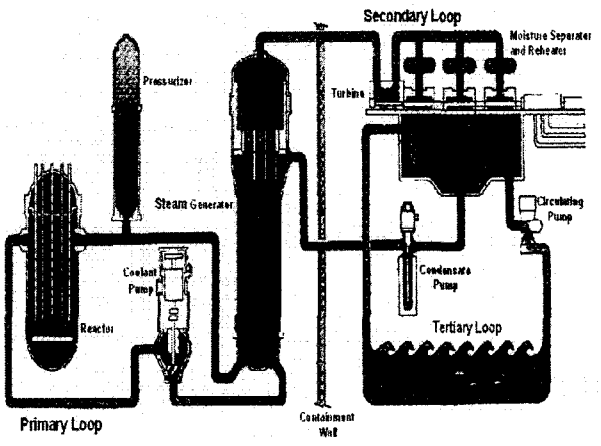

Fig. 2. Typical steam generator tubes in nuclear power plants (From an *Electric Power Research Institute (EPRI)* report)

The thermal energy transferred from the primary coolant causes the generation of steam which in turn is used for operating turbines. The harsh environmental conditions that exist within the steam generator

contribute to corrosion in the tube. The tubes have to be inspected periodically to ensure that the tubes are not causing nuclear contamination of the water on the secondary side. A popular inspection technique involves the use of ultrasonic NDE methods. In inspecting the steam generator tubes, the ultrasonic transducer moves along the tube axis with water sealed between the tube wall and the transducer. Figure 3 shows the ultrasonic inspection setup. The steam generator tube is anchored at one end to a thick ferromagnetic plate called the *tube sheet*. Figure 3 shows the tube in the *tube sheet* region. The tubes may contain cracks in this region. Such cracks usually extend 2 inches along the tube within and above the *tube sheet*.

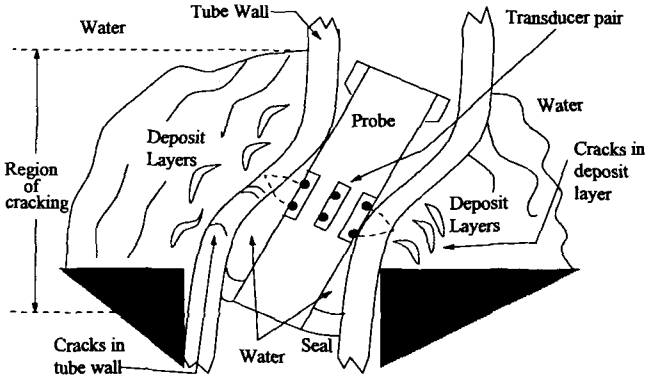

Fig. 3. Geometry of ultrasonic NDE of the steam generator tube

The tubes are expanded against the *tube sheet* and this may result in the occurrence of cracks. Additionally, chemical precipitates and dissolved metallic compounds are deposited on the tube sheet in this region. The accumulation and expansion of the deposit material produces localized bowing of the tube immediately above the *tube sheet* [11]. The transducers used in this inspection have nominal center frequencies of 8-11 MHz (within 6dB from ~6 to ~16 MHz). The sampling frequency is 80 MHz and the thickness of the tube wall is 0.047 inches. The transducer transmits longitudinal waves with a 19.5° incidence angle. The wave travels through the water and is incident on the inner wall of the tube as shown in Figure 4 which illustrates the travel paths of the wave. When the wave arrives at the tube inner wall, mode conversion occurs and the shear wave travels into the tube wall internally at a 45° refraction angle. Signals generated by the piezoelectric elements are sampled using an 8 bit converter at a sampling rate of 80 Mb/s.

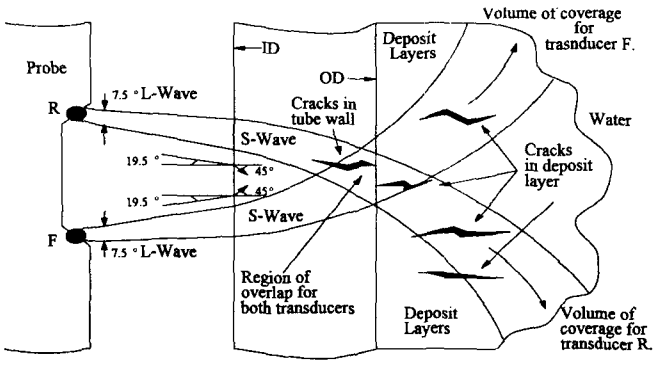

Fig. 4. Illustration of the signal collection

The sampled and digitized signal is a 482-point signal displayed in an A-Scan format. Note that each pair of transducers is composed of two elements (forward and reverse). The signals from the two transducers are combined to form a composite A-Scan consisting of 964 sample points. The A-Scans are combined along the tube axis to obtain a 2-dimensional B-Scan image for each pair of transducers. The ultrasonic wave can be scattered by cracks present in the tube or inhomogeneities present in the chemical precipitates and dissolved metallic compounds that are deposited outside.

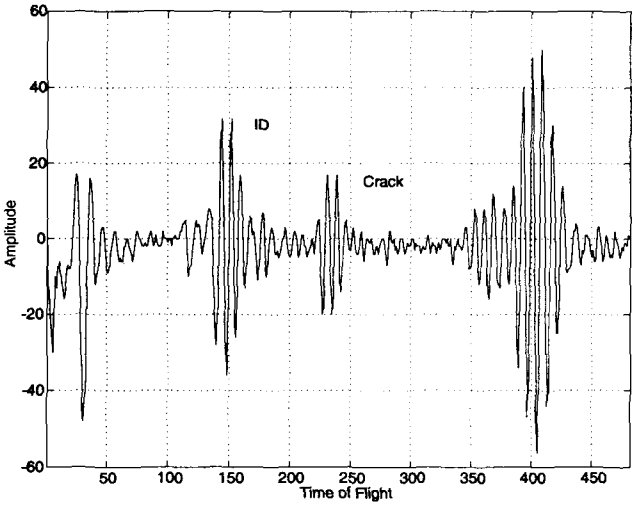

Fig. 5. A-Scan signal of a deposit from the forward transducer

The latter is benign and must be distinguished from cracks in the tube wall [12]. The B-Scan image consists of signal which may represent either cracks or deposits. The signals from cracks must be discriminated from those due to deposits, since cracks in the tube wall may result in leakage of the primary

coolant. The signals from deposits are, as indicated before, benign indications and are not a source of concern. Figures 5 shows the A-Scan signal from one of the cracks. The first and the third vertical strips with high amplitudes represent reflections from the inner diameter (ID) while the others (second and fourth) represent multiple-reflections from the ID. Figure 6 shows a one dimensional A-Scan signal from deposits. It is apparent that signals due to cracks and deposits are not significantly different. Discriminating these signals manually can be very slow and expensive. Consequently there is considerable interest in automatic methods for analyzing the data [13]. Automated

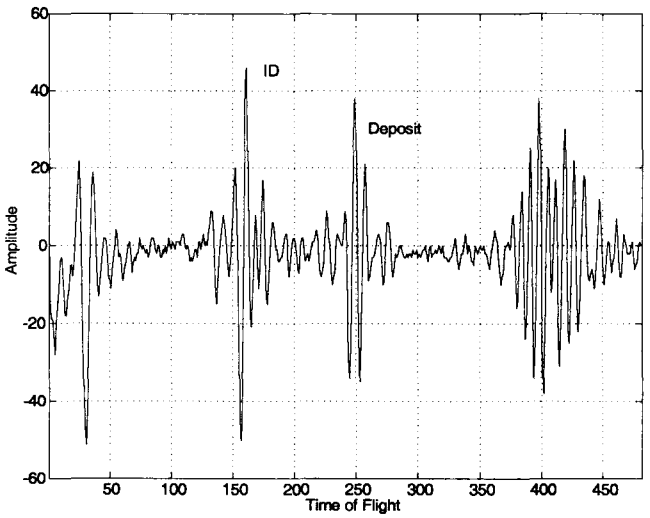

Fig. 6. A-Scan signal of a deposit from the forward transducer

methods offer such advantages as consistency of interpretation, rapid turnaround time and lower overall costs.

III. CLASSIFICATION USING A MODEL BASED DECONVOLUTION

In deconvolution problems, the pulse-echo wavelet needs to be estimated accurately since the estimation of the location of the scatterer relies on an accurate estimation of the location of the peak value of the echo [14]. Even a small error could have a significant impact on our ability to classify [10][15].

1. Deconvolution of Backscattered Echoes

The magnitude spectrum from the Fourier transform of the transducer pulse-echo wavelet shows bandpass characteristics. Therefore, the pulse-echo wavelet, $h(t)$, can be modelled as a sum of superimposed bandpass signals (Gaussian echo wavelet). In the time domain [10] :

$$h(t)=\sum_{m=0}^{M}\omega_m\, e^{-\alpha_m (t-\lambda_m)^2}\cos(2\pi f_m(t-\lambda_m)+\phi_m) \quad (1)$$

where M is the model order, ω_m is the weight, α_m is the bandwidth factor, λ_m is the time of flight, f_m is the center frequency, and ϕ_m is the phase of the corresponding pulse-echo wavelet. The parameters can be represented as a vector, $\vartheta_m=[\alpha_m\ \lambda_m\ f_m\ \phi_m\ \omega_m]$. We also assume that the signal contains additive white Gaussian noise (WGN). Then the pulse-echo wavelet, $h(t)$, can be written as

$$h(t)=\sum_{m=1}^{M} G(\vartheta_m;t)+v(t) \quad (2)$$

where $v(t)$ is a WGN process and $G(\vartheta_m;t)$ represents a Gaussian echo wavelet. Figure 7 shows an example of a pulse-echo wavelet generated by the model in equation (1).

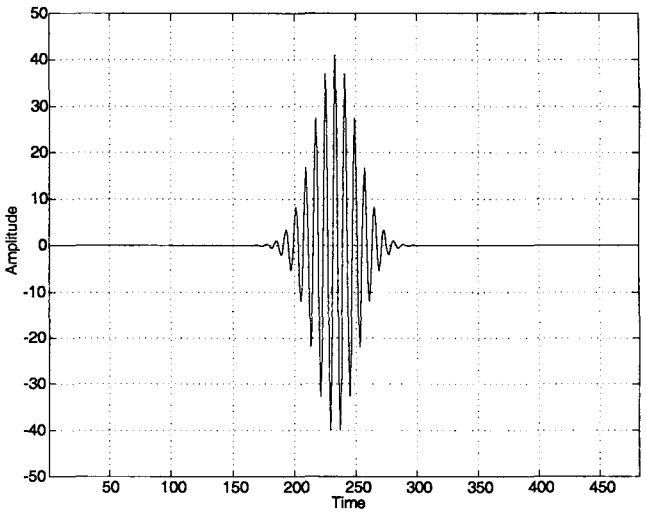

Fig. 7. A typical pulse-echo wavelet

The corresponding parameter vector is $[0.1\ 233\ 10^7\ 0\ 41]$. When an ultrasonic echo, $s(t)$, is propagated through a frequency independent homogeneous path and reflected from a flat surface, it

can be represented by the model

$$s(t)=\beta h(t-\tau) \tag{3}$$

where β is the amplitude, $h(t)$ denotes the transducer pulse-echo wavelet, and τ stands for the time of flight. Equation (3) means that the ultrasonic backscattered echo, $s(t)$, is the time-shifted and amplitude scaled version of the pulse-echo wavelet, $h(t)$. The amplitude of the backscattered echo, β, basically depends on the impedance, size or orientation of the scatterer and the time of flight of the echo, τ, is related to the location of the scatterer indicating the distance between the transducer and the reflector assuming that the velocity of ultrasound in the propagation path in the material is known. The transducer pulse-echo wavelet, $h(t)$, can be represented as a sum of a number of Gaussian echo wavelets. An ultrasonic backscattered echo, $y(t)$, reflected from an isolated target in a homogeneous and non-dispersive path, can be represented by equation (4) which is equivalent to stating that $y(t)$ is a sum of M echoes [10]

$$y(t)=\sum_{m=1}^{M}\beta_m h(t-\tau_m)+v(t) \tag{4}$$

where the reflectivity vector $\xi_m=[\beta_m \ \tau_m]$ represents the amplitude and the time of flight of the mth echo. The $v(t)$ in equation (4) stands for the measurement noise and can be characterized as WGN as described earlier. This model can represent M number of backscattered echoes from a localized target in a material assuming that the transducer pulse-echo wavelet is invariant throughout the propagation path. The model in equation (4) can be expressed as a deconvolution problem where the objective is to estimate the parameter vectors, ξ_m, from the observed backscattered echoes as follows

$$y(t)=h(t)*\left\{\sum_{m=1}^{M}\beta_m\delta(t-\tau_m)\right\}+v(t) \tag{5}$$

Here, $h(t)$ denotes the transducer pulse-echo wavelet, $v(t)$ is WGN, and the impulse train with δ function denotes the unknown system response. The objective is to estimate ξ_m based on a knowledge of $y(t)$. It is assumed that the desired system response is a spike train composed of unknown amplitudes and time of flights. Also, it is assumed that statistical knowledge about the amplitudes and locations of the desired system response is not
available. The model-based deconvolution problem is described next.

2. Newton-Raphson Method

In the estimation procedure, the Newton-Raphson algorithm has been developed and tailored to our specific problem for fast computation and convergence to estimate the time of flight and the distance between the tube wall and the ultrasonic sensors. The Newton-Raphson method is given by [16]

$$\zeta^{(k+1)}=\zeta^{(k)}-\mu\left(\frac{\partial^2 U(\zeta)}{\partial\zeta^2}\right)^{(-1)}\frac{\partial U(\zeta)}{\partial\zeta}\Big|_{\zeta=\zeta^{(k)}} \tag{6}$$

where $U(\cdot)$ is the objective function, μ is the convergence factor and ζ is the parameter to be estimated. The Newton-Raphson algorithm usually offers superior convergence properties, compared to the steepest descent algorithm [17]. The price is a computationally more demanding algorithm, since the Hessian needs to be computed and inverted [15][16]. The Newton-Raphson algorithm can be summarized as follows [18]:

(a) Choose an initial guess, $\zeta^{(0)}$

(b) Compute $\nabla_\zeta U$, which is, $\frac{\partial U(\zeta^{(0)})}{\partial\zeta}$

(c) Compute the Hessian, $\nabla_\zeta^2 U$, that is, $\frac{\partial^2 U(\zeta^{(0)})}{\partial\zeta^2}$

(d) Adjust $\zeta^{(0)}$ to obtain $\zeta^{(1)}$ by calculating,

$$\zeta^{(1)}=\zeta^{(0)}-\mu\left[\frac{\partial^2 U(\zeta^{(0)})}{\partial\zeta^2}\right]^{-1}\cdot\left[\frac{\partial U(\zeta^{(0)})}{\partial\zeta}\right]$$

(e) Stop when $\zeta^{(k+1)}-\zeta^{(k)}$ is sufficiently small.

The estimation procedure can be performed numerically

$$\zeta^{(k+1)}=\zeta^{(k)}-\Gamma\cdot\frac{U|_{\zeta=\zeta^{(k)}+\Delta\zeta}-U|_{\zeta=\zeta^{(k)}}}{\Delta\zeta} \tag{7}$$

where Γ is μ multiplied by the inverse of Hessian and

$\Delta\zeta$ is an appropriately small value. As indicated in equation (5), the observed echoes, $y(t)$, can be represented by the M number of superimposed pulse-echo wavelets and additive noise. We wish to estimate the amplitudes, β, and the locations, τ, by minimizing the MSE between the observed signals and the calculated signals using the Newton-Raphson method assuming the noise is WGN. Generally, the MSE is a nonlinear function of the parameters, β and τ. LMS methods often converge to local minima of the MSE hyper-surface. We use the expectation maximization (EM) algorithm along with the Newton-Raphson method to minimize the local convergence problem.

3. Expectation Maximization Algorithm

The expectation maximization (EM) algorithm is used to obtain the maximum-likelihood estimate (MLE) of the parameter, ξ_m [13]. The EM algorithm consists of two major steps. One is an expectation step and the other is a maximization step [11]. The expectation is with respect to the unknown underlying variables, using the current estimate of the parameters and conditioned upon the observations [19]. The maximization step then provides a new estimate of the parameters. These two steps are iterated until the estimate converges. However, the EM algorithm has a parallel computing structure which means that the expected signals are computed using the current estimate of parameter sets and the observed data at each step of the algorithm. After that, the corresponding parameter sets are computed using those expected signals. The parallel computing structure may sometimes affect the convergence rate of the estimation procedure. Alternatively, the parameter sets can be updated right after the maximization step without waiting for the other parameter vectors to be calculated. This step will incorporate the current estimated parameter vectors immediately into the expectation step and result in faster convergence. This method is known as the generalized EM algorithm and for the case of WGN, this method is known as the space alternating generalized EM (SAGE) algorithm [13]. Similar to the EM algorithm, the SAGE algorithm involves estimating an expected signal for each echo and then computing the MLE of the corresponding parameter set using the expected signal and the current value of parameters [12]. The flowchart of the algorithm is given in Figure 8. The SAGE algorithm solves the problem relating to the estimation of the parameters associated with M echoes by solving a one-echo estimation problem at each iteration [20].

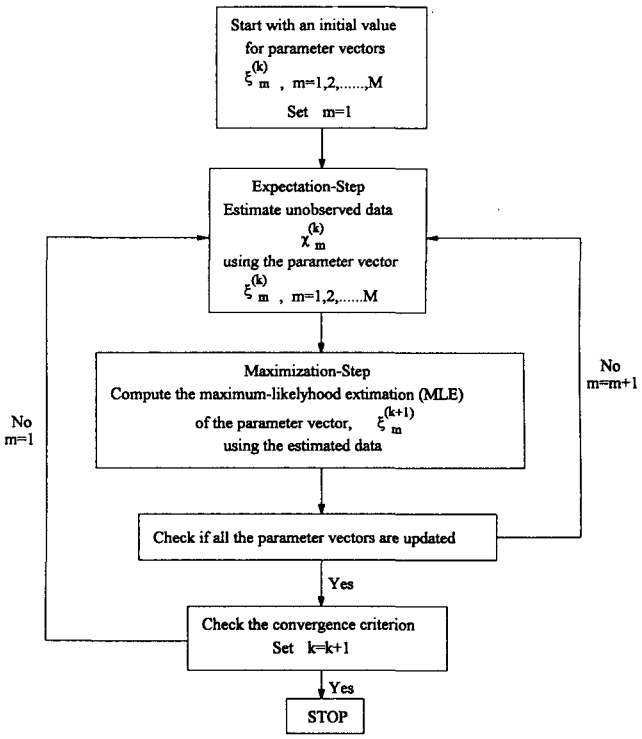

Fig. 8. Flowchart of the SAGE Algorithm

However, the convergence and speed of the SAGE algorithm depends on the convergence and speed of the maximization step in which the Newton-Raphson algorithm is employed. The convergence depends on the initial starting value and the degree of tendency to get stuck at local minima. The problem of convergence to a local minimum can be avoided by perturbing the solution and iterating again using the Newton-Raphson algorithm to continue the search for the global minimum. If the MSE is reduced in any direction among those tries, then the direction is chosen to keep searching for the global minimum. However, if there is no difference then the current minimum value is accepted as the global minimum. The convergence factor can be determined by inspecting the periodicity of the error function. The period of the local minima is close to the backscattered echo period, in other words, the inverse of the center frequency, f_c, for a single Gaussian echo or the inverse of the largest center frequency when there are multiple Gaussian echoes can be the period of the local minima. Therefore, in order

to avoid the local minimum value, $\frac{1}{2(f_c)_{\max}}$ can be chosen as the convergence factor, where the $f_{c\,\max}$ is the maximum center frequency among the center frequencies of multiple Gaussian echoes which compose the observed signal. The global search procedure should be performed in the Newton-Raphson algorithm to make sure the global convergence is reached in the maximization step. To summarize, the SAGE algorithm for estimating the amplitude, β, and location, τ, of the backscattered echoes involves the following steps.

Step 1. Start with making an initial guess for reflectivity vector, $\xi^{(0)}=[\beta^{(0)}, \tau^{(0)}]$ where, β =amplitude, and τ=time of flight. Set $k=0$ (iteration number).

Step 2. (Expectation Step) Compute

$$\hat{x}_m^{(k)} = s(\xi_m^{(k)}) + \frac{1}{M}\left\{y - \sum_{l=1}^{M} s(\xi_l^{(k)})\right\}$$

where, $s(\xi_m)=\beta_m h(t-\tau_m)$, and

$\xi_m=[\beta_m, \tau_m]$

Step 3. (Maximization Step) Iterate the parameter vector using the Newton-Raphson algorithm coupled with the global search procedure:

$$\xi_m^{(k+1)} = \arg_{\xi_m} \min \; || \hat{x}_m^{(k)} - s(\xi_m)||^2$$

and set $\xi_m^{(k)} = \xi_m^{(k+1)}$

Step 4. Set $m \rightarrow m+1$ and go to step 2 unless $m>M$

Step 5. Check convergence criterion: if $|| \xi^{(k+1)} - \xi^{(k)}|| \leq$ tolerance, then go to step 7 and stop, otherwise go to step 6.

Step 6. Set $m=1$, $k \rightarrow k+1$, and go to step 2.

Step 7. The estimated parameter vector is ξ.

The model order, M, is assumed to be one in the expectation step and the Newton-Raphson method is used in the maximization step. In step 3, the maximization procedure using the Newton-Raphson method can be implemented numerically with respect to the mth amplitude, β_m, and the mth time of flight, τ_m, respectively,

$$\beta_m^{(k+1)} = \beta_m^{(k)} - \Gamma \cdot \frac{Q_m \mid_{\beta_m=\beta_m^{(k)}+\Delta\beta_m,\ \tau_m=\tau_m^{(k)}} - Q_m \mid_{\beta_m=\beta_m^{(k)},\ \tau_m=\tau_m^{(k)}}}{\Delta\beta_m} \quad (8)$$

$$\tau_m^{(k+1)} = \tau_m^{(k)} - \Gamma \cdot \frac{Q_m \mid_{\tau_m=\tau_m^{(k)}+\Delta\tau_m,\ \beta_m=\beta_m^{(k)}} - Q_m \mid_{\tau_m=\tau_m^{(k)},\ \beta_m=\beta_m^{(k)}}}{\Delta\tau_m} \quad (9)$$

where Q_m is $|| \hat{x}_m^{(k)} - s(\xi_m)||^2$, Γ is μ multiplied by the inverse of Hessian and $\Delta\beta_m$, $\Delta\tau_m$ are appropriately small increments in the values of β_m and τ_m respectively. In this algorithm, making a good initial guess is important to obtain fast convergence. When the model order is one, *(M=1)*, a reasonable initial guess for TOF and the amplitude would be the time corresponding to the middle of the echo, and a value similar to the peak value of the echo, respectively.

IV. Results of the classification

Using the SAGE algorithm, the amplitude, β, and the location, τ, have been estimated. Figures 9 through 13 show the deconvolution results for cracks while figures 14 through 18 show the results for deposits. The estimated amplitude and TOF values are listed in tables 1 and 2 for cracks and deposits respectively. The pixel distance between ID (dotted stem) of the tube and the desired system response (solid stem) also has been listed in the tables so that it can be used as a basis of classification between cracks and deposits.

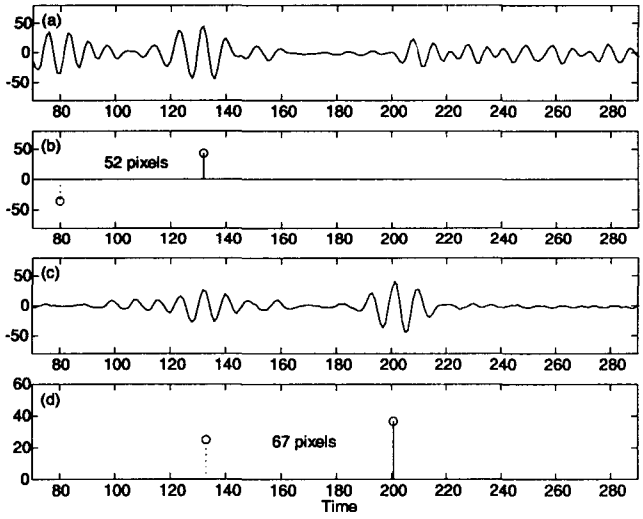

Fig. 9. Deconvolution results for cracks: (a)68%, (b)result for (a), (c)47%, (d)result for (c)

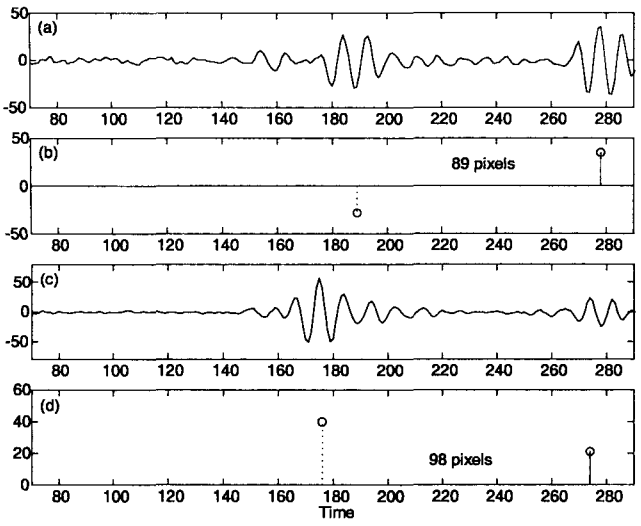

Fig. 10. Deconvolution results for cracks: (a)15%, (b)result for (a), (c)20%, (d)result for (c)

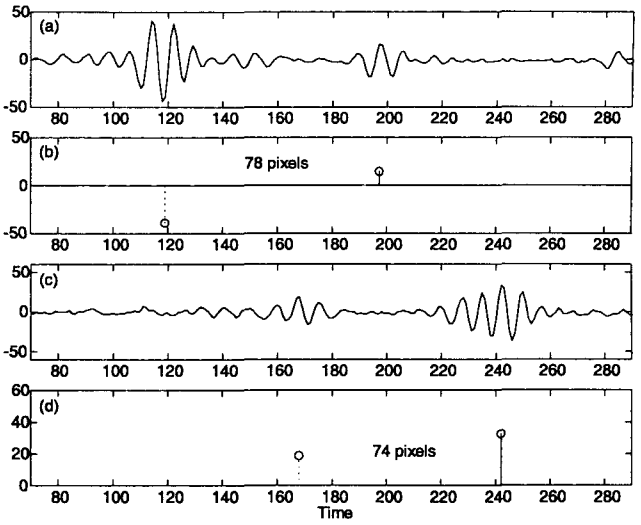

Fig. 12. Deconvolution results for cracks: (a)29%, (b)result for (a), (c)54%, (d)result for (c)

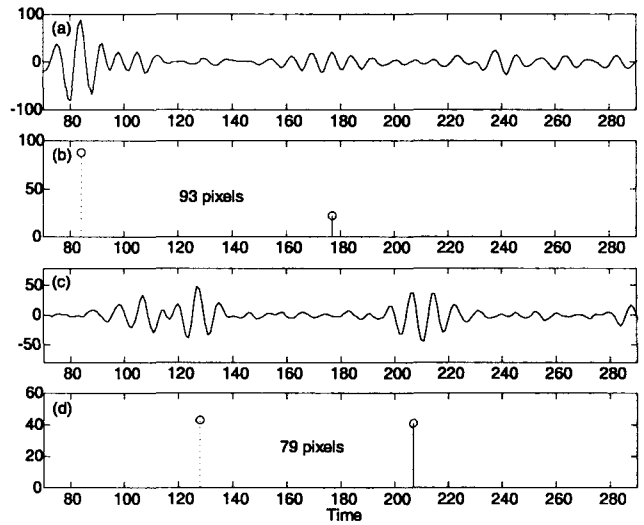

Fig. 11. Deconvolution results for cracks: (a)18%, (b)result for (a), (c)31%, (d)result for (c)

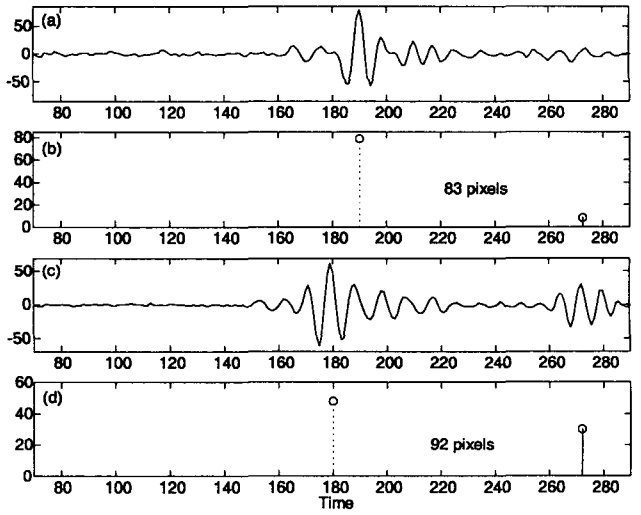

Fig. 13. Deconvolution results for cracks: (a)11%, (b)result for (a), (c)20%, (d)result for (c)

In each of the figures 9 through 18, (a) and (c) represent the observed ultrasonic backscattered echoes windowed around the echo from the ID of the tube and the target response from the scatterer, (b) and (d) represent the deconvolution results corresponding to the signals shown in (a) and (c) respectively. From these results, the % represents the amount of penetration of the cracks or depth of the deposits with respect to the thickness of the tube wall. The X- and Y-axis for each of the figures represent time and amplitude of the signal respectively. The backscattered echo from a crack and a deposit portion is windowed and applied to the algorithm to estimate β and τ. The dotted stem represents the amplitude and position of ID of the tube estimated and the solid stem represents the amplitude and position of the desired system response estimated from the model based deconvolution. From the B-Scan image of the ultrasonic data, it is known that the distance between ID and OD is approximately 89 pixels with a 45° refraction angle at ID, therefore, the estimated distance between the dotted stem and solid stem can be used to determine if it is a crack in the tube or a inhomogeneity in deposit layer. If the distance is less than 89 then it is classified as a crack in the tube, otherwise it is classified as a inhomogeneity in deposit layer.

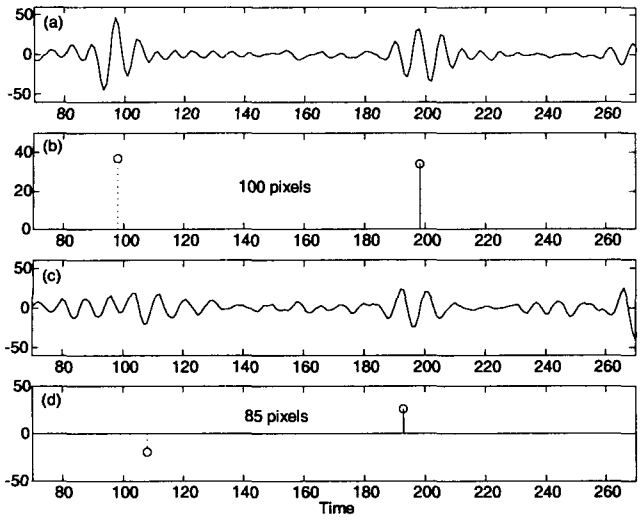

Fig. 14. Deconvolution results for deposits: (a)45%, (b)result for (a), (c)40%, (d)result for (c)

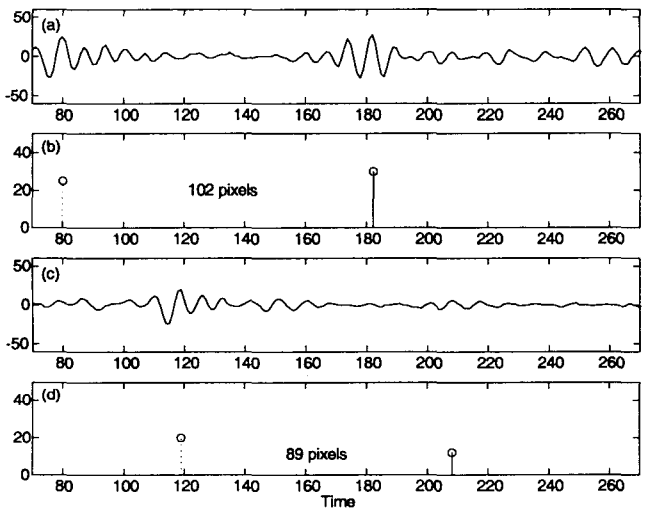

Fig. 15. Deconvolution results for deposits: (a)18%, (b)result for (a), (c)8%, (d)result for (c)

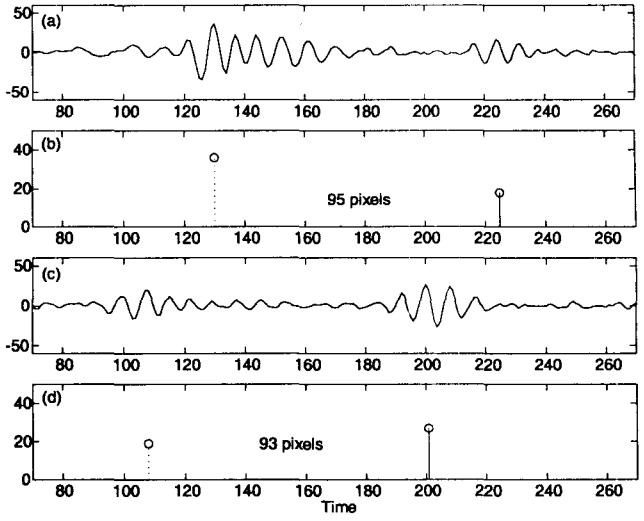

Fig. 16. Deconvolution results for deposits: (a)10%, (b)result for (a), (c)17%, (d)result for (c)

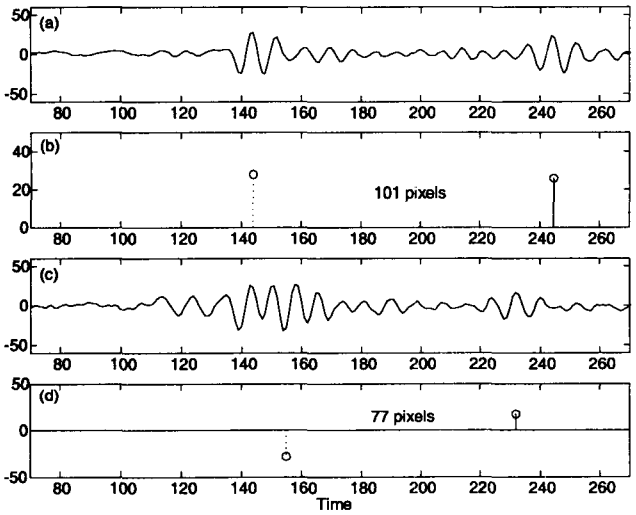

Fig. 17. Deconvolution results for deposits: (a)29%, (b)result for (a), (c)45%, (d)result for (c)

This method may produce incorrect classification results unless the position of the scatterer is estimated with high resolution. The estimated β, τ, and the distance between ID of the tube and the target response are listed in tables 1 and 2. The initial value of β and τ for the iterations in the SAGE algorithm are chosen to be the peak amplitude and the time of flight of the input ultrasonic backscattered echoes respectively. The number of iterations of the SAGE algorithm is relatively small compared to the steepest descent algorithm. This saves processing time since the SAGE algorithm uses the information contained in the Hessian while the steepest descent algorithm uses only the gradient information.

V. Conclusions

A novel approach to the classification of ultrasonic nondestructive evaluation (NDE) signals has been described in this thesis. The method uses a least mean square (LMS) algorithm and the results obtained using the new approach were described with those obtained using the space alternating generalized expectation maximization (SAGE) algorithm in conjunction with the Newton-Raphson method.

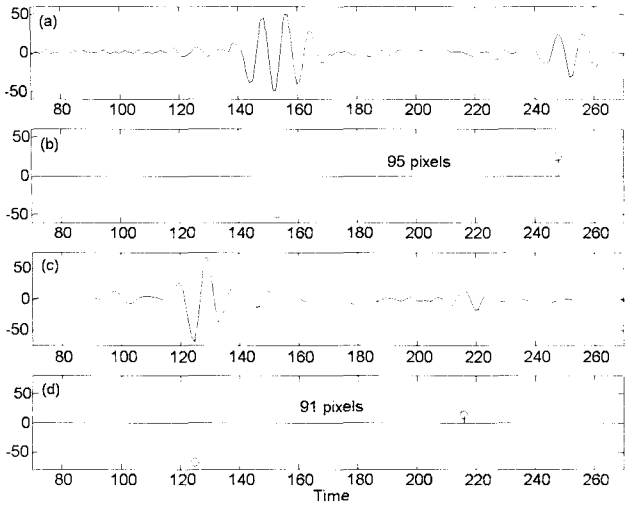

Fig. 18. Deconvolution results for deposits: (a)33%, (b)result for (a), (c)38%, (d)result for (c)

Cracks	Amp.	TOF	Distance
68%	43.3010	132	52
47%	36.8673	201	67
15%	35.1328	278	89
20%	21.1184	274	98
18%	22.0650	177	93
31%	40.9272	207	79
29%	14.6779	197	78
54%	32.6396	242	74
11%	8.1381	273	83
20%	30.1390	272	92

Table 1. Estimated values of the amplitude, β, and TOF, τ, from the model based deconvolution technique for cracks

The classification has been performed using data from the straight and bent portions of the tube. The results obtained have been described with those obtained using a model based deconvolution approach. The transducer pulse-echo wavelet has been modelled and estimated in terms of Gaussian echo wavelets. The observed ultrasonic backscattered echoes are also modelled as the convolution of the pulse-echo wavelet with the desired system response. The amplitude and the time of flight (TOF) of the desired system response have been estimated using the space alternating generalized expectation maximization (SAGE) algorithm in conjunction with the Newton-Raphson method. The scatterer location estimates are used as a basis for classification. Additional work in the future can be focused on reducing the computation time.

Deposits	Amp.	TOF	Distance
45%	33.9559	198	100
40%	26.4823	193	85
18%	29.9457	182	102
8%	12.3617	208	89
10%	18.3612	225	95
17%	27.9343	201	93
29%	25.9780	245	101
45%	16.7784	232	77
33%	24.1351	248	95
38%	13.6415	216	91

Table 2. Estimated values of the amplitude, β, and TOF, τ, from the model based deconvolution technique for deposits

접수일자 : 2002. 12. 18 수정완료 : 2003. 1. 19

VI. References

[1] W. H. Hayt, Jr., Engineering Electromagnetics, *McGraw-Hill Book Company, New York,* 1989.

[2] D. E. Bray, R. K. Stanley, Nondestructive Evaluation, *CRC Press Inc., Boca Raton,* 1997.

[3] L. W. Schmerr, Jr., Fundamentals of Ultrasonic Nondestructive Evaluation, *Plenum Publishing Corporation, New York,* 1998.

[4] Nondestructive Testing Encyclopedia, The e-Journal of Nondestructive Testing, last viewed June 2001., *Available at http://www.ndt.net/article/az/ut_idx.htm.*

[5] Nondestructive Testing Encyclopedia, The e-Journal of Nondestructive Testing, last viewed June 2001.,

[6] A. Khan, Defect Classification for Steam Generator Tubes of a Nuclear Power Plant using Ultrasonic Nondesstructive Techniques, *M. S. Thesis, Iowa State University,* 2001.

[7] M. Feder, E. Weinstein, Parameter Estimation of Superimposed Signals using the EM Algorithm, *IEEE Transactions on Acoustic Speech Signal Processing*, vol. 36, no.4, pp. 477-489, April 1988.

[8] J. A. Fessler, A. O. Hero, Space Alternating Generalized Expectation Maximization Algorithm, *IEEE Transactions on Signal Processing*, vol. 42, no. 10, pp. 2664-2677, October 1994.

[9] R. Demirli, J. Saniie, Model-Based Estimation of Ultrasonic Echoes, Part I: Analysis and Algorithms, *IEEE Transactions on Ultrasonics, Ferroelectrics, and Frequency Control*, vol. 48, no. 3, pp.787-802, May 2001.

[10] R. Demirli, J. Saniie, Model-Based Estimation of Ultrasonic Echoes, Part II: Nondestructive Evaluation Applications, *IEEE Transactions on Ultrasonics, Ferroelectrics, and Frequency Control*, vol. 48, no. 3, pp. 803-811, May 2001.

[11] R. Xing, Ultrasonic NDE signal classification on steam generator tubes, *M.S. Thesis, Iowa State University*, 2000.

[12] D. R. Prabhu, M. N. Abedin, W. P. Winfree, E. I. Madaras, Disbond detection through ultrasonic signal classification using an artificial neural network, *International Joint Conference on Neural Networks*, Vol.2, pp.906, 1991.

[13] R. Schalkoff, Pattern Recognition, *John Wiley & Sons, Inc, New York*, 1992.

[14] J. S. DaPonte, J. Gelber, M. D. Fox, Statistical classification of ultrasonic image texture, *Proceedings of the 15th Annual Northeast Bioengineering Conference*, pp.121-122, 1989.

[15] J. M. Mendel, Optimal Seismic Deconvolution: An Estimation-Based Approach, *NY: Academic Press*, 1983.

[16] S. M. Kay, Fundamentals of Statistical Signal Processing, *Prentice-Hall, Englewood Cliffs*, 1993.

[17] V. Solo, X. Kong, Adaptive Signal Processing Algorithms, *Prentice Hall, Englewood Cliffs*, 1995.

[18] P. S. R. Diniz, Adaptive Filtering, *Kluwer Academic Publishers, Norwell*, 1997.

[19] T. K. Moon, The expectation-maximization algorithm, *IEEE Signal Processing Magazine*, pp. 47-60, Nov. 1996.

[20] A. M. Sabatini, A digital signal processing technique for ultrasonic signal modeling and classification, *IEEE Transactions on Instrumentation and Measurement*, Vol.50, No.1, pp.15-21, Feb. 2001.

김대원 (Daewon Kim)
正會員
1993년 2월 중앙대학교 전자공학과 (공학사)
1993년 1월 - 1993년 10월 삼성전자 연구원
1996년 5월 University of Southern California (M.S.)
2002년 5월 Iowa State University (Ph. D.)
2002년 5월 - 현재 삼성전자 통신연구소 책임연구원
관심분야: 영상신호처리, 영상압축, 영상인식, Neural Network, Ultrasonic NDE 신호처리